ELSEVIER

Orientation discrimination in human vision:
Psychophysics and modeling

William H.A. Beaudot [a,b,*], Kathy T. Mullen [a]

[a] McGill Vision Research, Department of Ophthalmology, McGill University, 687 Pine Avenue West, H4-14, Montréal, Que., Canada H3A 1A1
[b] KyberVision Consulting, R&D, 2150 Mackay Street, Suite 1908, Montréal, Que., Canada H3G 2M2

Abstract

We evaluated orientation discrimination thresholds using an external noise paradigm. Stimuli were spatiotemporal Gaussian patches of 2D orientation noise band-pass filtered in Fourier domain. Orientation acuity was measured for various combinations of stimulus spatial bandwidth, spatial frequency, and size as a function of orientation bandwidths of the stimuli. Stimulus contrast was matched in multiples of detection threshold. Consistent with the idea that stimulus orientation bandwidth acts as a source of external noise, orientation discrimination thresholds increased monotonically in all conditions with stimulus bandwidth. To interpret these results quantitatively, we first fitted a variance summation model to the data and derived the internal orientation noise, relative sampling efficiency, and orientation tuning of the mechanism underlying orientation discrimination. Due to the equivocal biological nature of these parameters for orientation discrimination, we investigated, with a modeling approach, how neural detectors characterized by a broad orientation tuning may support orientation discrimination. We demonstrated using the ideal-observer theory that while linear models, based on either unimodal filtering or center-surround opponency, predict the monotonic relationship between orientation discrimination threshold and orientation noise, a nonlinear model incorporating a broadband divisive inhibition in the orientation domain is a better candidate due to its contrast invariance. This model, using broad and similar orientation tuning for its excitatory and inhibitory inputs, accounts for the acute orientation acuity of human vision and proves to be robust despite the variance found in natural stimuli.
© 2005 Elsevier Ltd. All rights reserved.

Keywords: Orientation discrimination; Gain control model; Orientation selectivity; Human vision

1. Introduction

Early visual processing is characterized by neural and psychophysical mechanisms that are broadly tuned for wavelength, spatial frequency, orientation, and other visual attributes. For example, neurophysiological evidence indicates a broad orientation tuning (full-bandwidth at half-height, FBHH ≈ 40–60 deg) in cortical visual cells in both monkeys and cats (Blake & Holopigian, 1985; De Valois, Yund, & Hepler, 1982; Hammond & Andrews, 1978; Heggelund & Albus, 1978; Vogels & Orban, 1991). Masking

and adaptation paradigms used to investigate orientation selectivity in human vision also support this broad orientation tuning for detection tasks (FBHH ≈ 30–60 deg) (Blake & Holopigian, 1985; Pandey Vimal, 1997; Phillips & Wilson, 1984). The visual system is nevertheless astonishing in its capacity to discriminate very small variations in the image content, for example in terms of color, position, orientation, curvature, and stereopsis. In particular, human vision is characterized by acute orientation discrimination, typically less than 1 deg, despite the evidence for broad orientation tuning of the underlying detectors (Burr & Wijesundra, 1991; Regan & Beverley, 1985; Webster, De Valois, & Switkes, 1990).

A differential-response model of orientation discrimination has been proposed to solve this apparent discrepancy

* Corresponding author. Tel.: +1 514 245 0714; fax: +1 514 843 1691.
E-mail address: william.beaudot@kybervision.net (W.H.A. Beaudot).

and to account for the off-looking strategy used by the visual system to detect orientation change (Regan & Beverley, 1985; Wilson & Regan, 1984). According to this model, formulated either as a line-element or an opponent-process model, orientation thresholds are not limited by the tuning bandwidth of the underlying detectors but by their ability to turn a stimulus orientation change into a reliable response change. This response is maximal where the slope of the tuning curve is the steepest. In such models, the steepness of the slope of the tuning curve and noise levels limit orientation resolution. A corollary of this model, called an off-looking strategy, is that the most sensitive detectors to orientation change are not the most activated ones (i.e., those with the stimulus orientation close to the detector orientation peak), but are those with a more remote orientation peak (Regan & Beverley, 1985; Wilson & Regan, 1984). The plausibility of such a model has been demonstrated neurophysiologically in both cats and monkeys (Bradley, Skottun, Ohzawa, Sclar, & Freeman, 1985, 1987; Geisler & Albrecht, 1997; Scobey & Gabor, 1989; Vogels & Orban, 1990). Despite their broad orientation tuning, single neurons in the primary visual cortex can reliably signal orientation differences of about 1 deg, and it is the slopes of their tuning curves and response variability that determine the minimum orientation differences that can elicit a reliable response change.

Models that have attempted to account for orientation discrimination, such as the line-element model (Wilson & Regan, 1984) and opponent-process model (Regan & Beverley, 1985), have implicitly considered grating-like stimuli with a narrow orientation tuning that contain ideally only one orientation. More natural and ecological stimuli, however, are texture-like with a broad orientation tuning. Moreover, stimuli may be either limited in size, or perceived by detectors with a limited spatial extent, both conditions having the effect of broadening the orientation content of the perceived stimuli. Thus, it is advantageous for the visual system to remain relatively insensitive to variation in the stimulus orientation bandwidth, and maintain a good sensitivity to orientation change despite the presence of orientation "uncertainty."[1]

In this paper, we combine a psychophysical and a modeling approach to address the issue of how the visual system can maintain acute orientation discrimination over a range of stimulus bandwidths, with the assumption of detectors with broad orientation tuning. In the psychophysical section of the paper, we re-evaluate orientation discrimination using an external noise paradigm. We first

measure orientation discrimination thresholds as a function of orientation bandwidth of the stimuli for various combinations of spatial bandwidth, spatial frequency, and size. To quantify the role of these spatial parameters on orientation discrimination, we fit the variance summation model to the data to derive the internal orientation noise, relative sampling efficiency, and orientation tuning of the underlying mechanism. We then use a modeling approach with the aim of explaining how neural detectors characterized by a broad orientation tuning can support acute orientation discrimination despite the presence of orientation noise in the stimuli. To our knowledge, no model based on the broad orientation tuning of the detection mechanisms has yet been proposed to account for the effect of the stimulus orientation bandwidth on orientation discrimination thresholds.

We consider two kinds of plausible "neural" model, linear and nonlinear, and predict their differential response to stimuli differing in mean orientation, similar to those presented in the psychophysical task. Using the ideal-observer theory we find that while linear models, based on either unimodal filtering or center-surround opponency, can account for the increase in orientation discrimination thresholds as a function of stimulus orientation bandwidth, they are not as robust as a nonlinear model that incorporates a broadband divisive inhibition in the orientation domain. This nonlinear model better accounts for the monotonic relationship between orientation discrimination and orientation bandwidth we find experimentally, especially in presence of contrast variation. By fitting the models to the experimental data, we derive estimates of the models' parameters, in particular the orientation bandwidths. The nonlinear model for orientation discrimination demonstrates its ability to predict the acute orientation acuity found in human vision despite the broad orientation tuning of its excitatory and inhibitory inputs. Finally, the relation between the variance summation model and the nonlinear model is discussed, as well as the biological plausibility of the proposed model.

2. Methods

2.1. Stimuli

Following previous studies (Beaudot & Mullen, 2002, 2005; Heeley, Buchanan-Smith, Cromwell, & Wright, 1997), we estimated orientation acuity for two-dimensional band-pass filtered noise. The stimuli are constructed by filtering Gaussian noise in the Fourier domain with an appropriate anisotropic filter. The modulation transfer function of this filter is a Gaussian in radial frequency and radial angle. The spectral density of the resulting noise can be expressed in polar coordinates:

$$S_n(f_x, f_y) = G_r(f_r, f_o, \sigma_f) \cdot G_\theta(\theta, \theta_o, \sigma_\theta), \tag{1}$$

where

$$G_r(f_r, f_o, \sigma_f) = \exp\left[-\frac{1}{2} \cdot \left(\frac{f_r - f_o}{\sigma_f}\right)^2\right], \tag{2}$$

---

[1] The external source of orientation uncertainty results from the orientation noise contained in the stimuli. Due to the broadband nature of the stimuli, this external orientation noise is quantified by either the variance or bandwidth of the orientation distribution. Consequently we use the terms 'orientation noise' and 'orientation bandwidth' to express the uncertainty produced by the orientation variance in the stimuli.
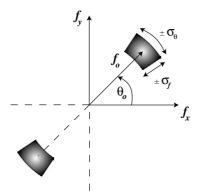
2D ORIENTED NOISE IN FOURIER DOMAIN

Fig. 1. Schematic Fourier representation of the spectral density of 2D oriented Gaussian noise.

$$G_\theta(\theta, \theta_o, \sigma_\theta) = \exp\left[-\frac{1}{2}\cdot\left(\frac{\theta-\theta_o}{\sigma_\theta}\right)^2\right]$$
$$+ \exp\left[-\frac{1}{2}\cdot\left(\frac{\theta-(\theta_o+\pi)}{\sigma_\theta}\right)^2\right], \quad (3)$$

$$f_r = \sqrt{f_x^2 + f_y^2}, \quad (4)$$

and

$$\theta = \mathrm{atan}(f_y/f_x), \quad (5)$$

f_x and f_y are the cartesian spatial frequencies, f_r is the radial spatial frequency, f_o is the peak spatial frequency, σ_f characterizes the frequency bandwidth, θ is the radial angle, θ_o is the peak (or mean) orientation, σ_θ characterizes the orientation bandwidth (half-bandwidth at half-height is given by sqrt$(2\cdot\ln(2))\cdot\sigma$). Fig. 1 illustrates the extent and location of the noise spectral density in the Fourier domain.

After inverse Fourier transform, the filtered noise $s_n(x,y)$ is multiplied by a spatiotemporal Gaussian envelope to obtain patches of orientation noise $s(x,y,f)$ localized in space-time
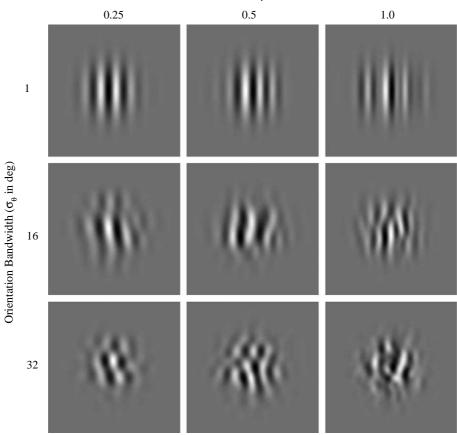
$$s(x,y,t) = s_n(x,y)\cdot g_r(x,y,x_o,y_o,\sigma_r)\cdot g_t(t,t_o,\sigma_t), \quad (6)$$

where $g_r()$ denotes a 2D Gaussian envelope centered at position (x_o,y_o) with a spread σ_r, and $g_t()$ denotes a temporal Gaussian envelope centered on time t_o with a time constant σ_t ($\sigma_t = 250$ ms).

Fig. 2 shows examples of the resulting noise stimuli, and illustrates the effects of increasing spatial and orientation bandwidths. The spatial parameters (f_o, σ_f, σ_r) were varied across the stimuli condition in the psychophysical experiment.

2.2. Apparatus and calibrations

Stimuli were displayed on a Sony Trinitron monitor (GDM-F500R) driven by a VSG 2/4F graphics board (Cambridge Research Systems, Rochester, England) with 15 bits contrast resolution, housed in a Pen-

GAUSSIAN-ENVELOPED 2D NOISE
Spatial Bandwidth (σ_f in octaves)

Fig. 2. Examples of noise stimuli: Gaussian-enveloped 2D noise as a function of spatial and orientation bandwidths.

tium PC computer. The frame rate of the display was 76 Hz. The monitor was gamma corrected in software with lookup tables using luminance measurements obtained with an OptiCAL gamma correction system interfaced with the VSG display calibration software (Cambridge Research Systems, Rochester, England). Luminance contrast was defined in cone contrast space (Cole & Hine, 1992; Sankeralli & Mullen, 1996). The monitor was viewed in a blacked out room. The mean luminance of the display was 60 cd/m². The stimuli were viewed at 60 cm. Stimuli were generated on-line, and a new stimulus was generated for each presentation.

2.3. Protocol

Orientation acuity (discrimination thresholds, σ_o) was measured at various combinations of spatial bandwidth (0.25–1 octaves), spatial frequency ($f_o = 1.5$–18 cpd), and size ($\sigma_r = 0.25$–1 deg) of the patches of orientation noise. All stimuli were matched in multiples of the contrast detection threshold, measured using a temporal 2AFC staircase procedure. In each trial, one interval contained a noise patch and the other contained a blank stimulus with the same average luminance. Subjects were asked to indicate which interval had the noise patch. Orientation discrimination was measured using another temporal 2AFC staircase procedure, at 10 times the contrast threshold measured in the first experiment as a function of the orientation bandwidth ($\sigma_\theta = 1$–48 deg) of the stimuli. The orientation bandwidth, defined by a Gaussian distribution with standard deviation σ_θ, can be considered as a source of external noise to explore the degree of selectivity of orientation tuning in the discrimination task. In each trial, the subject has to determine in which direction, clockwise or counter-clockwise, the patch of orientation noise in the second interval appeared to be rotated with respect to the first. One of the intervals contained a vertical reference patch with a ± 5 deg jitter ($\theta_o = 90 \pm 5$ deg), while the other one contained another noise patch rotated by a relative amount depending on the staircase. Both patches were independently generated.

In both 2AFC staircase procedures, either the stimulus contrast or the stimulus orientation difference was reduced after two correct responses, and increased after one wrong response. The change was 50% before the first reversal, and 25% after the first reversal. Each session stopped after six reversals, and the threshold corresponding to a criterion of 71% correct was computed from the mean of the last five reversals. The duration of each stimulus was 1 s, and the overall contrast of each stimulus was modulated in time up and down according

to a temporal Gaussian envelop ($\sigma_t = 250$ ms) centered on the temporal window (1 s). Auditory feedback was given after each trial. A black fixation mark was briefly presented at the beginning of each session in the center of the display, and subjects were asked to sustain their focus during the whole session. Practice trials were run before the experiments commenced. The number of trials per session was for each experiment between 30 and 50 for each subject, and 4–5 sessions were performed for each condition.

2.4. Observers

The observers were the two authors (WB and KTM). Both subjects have normal, or refracted to normal vision. All experiments were done under binocular conditions.

2.5. Models

2.5.1. Variance summation model

Typically, orientation discrimination thresholds increase monotonically with stimulus bandwidth. The manner in which orientation acuity declines with stimulus bandwidth suggests it is determined by a summation of noise processes (Pelli, 1990; Pelli & Farell, 1999), and so we fitted orientation discrimination thresholds with a variance summation model similar to previous studies (Beaudot & Mullen, 2002, 2005; Demanins, Hess, Williams, & Keeble, 1999; Heeley et al., 1997)

$$\sigma_o = \sqrt{\sigma_{Int}^2 + \frac{\sigma_\theta^2}{N}} \tag{7}$$

and

$$\sigma_{knee} = \sqrt{N} \cdot \sigma_{Int}. \tag{8}$$

According to this model illustrated in Fig. 3A, psychophysical thresholds are limited by both internal and external noise processes. These noise processes are assumed to be independent, thus their variances add. In this model, σ_o is the experimentally observed threshold, σ_{Int} is the internal noise, σ_θ is the external noise (stimulus orientation bandwidth in our experiment), and N is the sampling efficiency, which reflects how much of the stimulus is used for the task. A parameter of interest is the knee point of the curves (σ_{knee}), also called equivalent input noise, where the external and internal noises

VARIANCE SUMMATION MODEL

A Orientation Discrimination Threshold
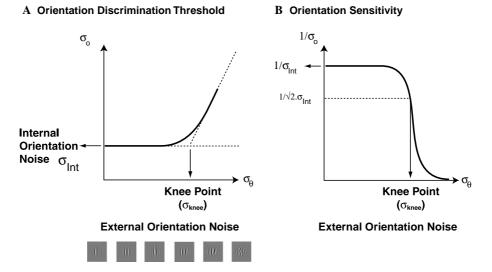
B Orientation Sensitivity

Fig. 3. Variance summation model: orientation discrimination threshold (A) and orientation sensitivity (B) as a function of external orientation noise, as predicted by Eq. (7).

make an equal contribution to the observed threshold. The meaning of this parameter appears clearer when representing orientation sensitivity instead of orientation threshold as a function of external orientation noise. As illustrated on Fig. 3B, it expresses the overall degree of orientation tuning of the discrimination mechanism. Our threshold data were fitted with this model using a least-squares procedure to derive the internal orientation noise, sampling efficiency, and orientation tuning (σ_{knee}).

2.5.2. Neural models

We next present two kinds of plausible neural model (illustrated in Fig. 4) whose aim is to relate the properties of a population of orientation-selective detectors to the perception of orientation in terms of detection and discrimination. We assume that orientation detection and discrimination are subserved by the response of individual detectors and their differential response, respectively. We consider an ensemble of orientation-selective detectors whose orientation tuning curves peak at different values that span homogeneously the full range of orientation (1D orientation ring), similar to the pinwheel structure found in the primary visual cortex (V1). This ensemble constitutes a set of identical broadband detectors with overlapping curves sampling the orientation domain at constant intervals (1 deg step). The orientation selectivity of the detectors is primarily set by a linear input stage with an orientation tuning defined by a Gaussian function (other types may be used, see Swindale, 1998). We considered a 2D spatial (Gabor-like) receptive field for this linear stage to ensure the interdependence of orientation selectivity and spatial extent.

The two types of models we investigated are distinguished by the processing following the linear input stage: (i) a center-surround quasi-linear model where the output of the linear stage may receive a surround inhibition in the orientation domain before applying a half-wave rectification and a Naka–Rushton equation used to model the contrast response function of striate cortex neurons (contrast gain control); and (ii) a nonlinear model incorporating a broadband divisive inhibition in the orientation domain. Note that in both models the response of the linear input stage is proportional to stimulus contrast. We consider

only static (i.e., steady state) versions of the models. Each model is simulated on the actual 2D stimuli used in the psychophysical experiment (orientation noise patches), and the ideal-observer theory is applied to their responses to predict their orientation discrimination performance. The predicted performances are fitted to the experimental data (orientation discrimination threshold versus stimulus orientation bandwidth) to obtain estimates of the models' parameters. We then compare the models' ability to account for the experimental data, and the predicted orientation bandwidths obtained from the fitting procedure.

2.5.2.1. Model stimuli. For consistency with our psychophysical data, our models use spatially identical but static stimuli, orientation noise patches as described in Eqs. (1)–(6). Stimuli all have the same mean luminance (0.5) and their maximum contrast is normalized (to unity) as the psychophysical stimuli were matched in multiples of contrast detection threshold and stimulus bandwidth has no or a small effect on contrast detection threshold. Note that the contrast normalization has a profound effect on the stimuli spectrum amplitude: the Fourier peak amplitude decreases exponentially with the stimulus orientation bandwidth ($\lambda(\sigma_\theta) = [\alpha + \beta \cdot \exp(-\sigma_\theta/\gamma)]/(\alpha+\beta)$) provides a good fit). Note also that the stimuli could not be simply modeled with a 1D Gaussian distribution in the orientation domain because of their stochastic nature (due to their random spatial phase) and their limited spatial extent that affects their actual orientation bandwidth.

Each 2D stimulus $s(x,y)$ is a function of five parameters, f_o its peak spatial frequency, σ_f its frequency bandwidth parameter, σ_r its space constant, θ_s its mean orientation, and σ_θ its orientation bandwidth parameter. As f_o, σ_f, and σ_f are fixed for a particular stimulus condition, we note $s(\theta_s, \sigma_\theta)$ the spatial stimulus with peak orientation θ_s and orientation bandwidth parameter σ_θ. For each stimulus condition, we pre-compute the first stage's response to a whole set of stimuli. The stimulus peak orientation (θ_s) is varied from 1 to 180 deg (by step of 1 deg) while the filter orientation is fixed (at 90 deg) to characterize the effect of the relative orientation between the two. The orientation bandwidth (characterized by σ_θ), which acts as a
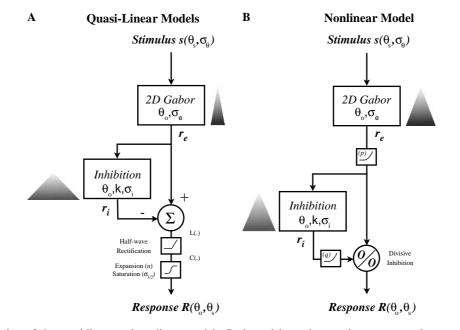

Fig. 4. Schematic description of the quasi-linear and nonlinear models. Both models receive two inputs, one excitatory and one inhibitory, which interact either linearly (A) or nonlinearly (B) to produce the response of the orientation-selective detector. The stimulus is defined by its peak orientation (θ_s) and its orientation bandwidth parameter (σ_θ). The detector response depends on the relative orientation between its tuning peak (θ_o) and the stimulus (θ_s).

source of external orientation noise, is varied as well from 1 to 48 deg (in steps of 1 deg). These 180×48 stimuli (# stimulus orientations $\times$ # stimulus orientation bandwidths) are regenerated for each orientation bandwidth of the input stage's filter.

2.5.2.2. Linear input stage (excitatory input). The linear input stage is a 2D Gabor filter with an even profile similar to the oriented receptive field found in VI simple cells (Jones & Palmer, 1987). Its response to a stimulus $s(x, y)$ is given by their 2D convolution

$$r_{\theta,\sigma}(x, y) = g_{\theta,\sigma}(x, y) *_{x,y} s(x, y), \qquad (9)$$

where $g_{\theta,\sigma}(x, y)$ denotes the filter impulse response with peak orientation θ and orientation bandwidth parameter σ (peak spatial frequency and spatial bandwidth were chosen to be the same than those of the stimuli). For the sake of simplicity, we only consider the location receiving the strongest response from the linear stage:

$$r = \text{Max}_{x,y}[r_{\theta,\sigma}(x, y)]. \qquad (10)$$

We note $r_e(\theta, \theta_s)$ the response of this linear stage characterized by an orientation bandwidth parameter σ_e and with peak orientation θ in response to a stimulus with a peak orientation θ_s, which constitutes the excitatory input signal of the subsequent processing. In all simulations, the orientation of the filter is fixed ($\theta = 90$ deg) and the stimulus mean orientation is varied from 0 to ± 90 deg relatively to θ, which provides the filter response as function of the relative orientation between the filter and the stimulus. Note that the response of this linear stage to a single stochastic stimulus is characterized by a Gaussian distribution in the orientation domain, a property we take advantage of for simulation purpose (see Appendix A for computational details).

2.5.2.3. Inhibitory input. The inhibitory component used for both center-surround quasi-linear model and nonlinear model consists of a 1D weighting function that describes the interaction between neighboring detectors in the orientation domain. The orientation tuning of this inhibitory component is also characterized by a Gaussian distribution $f(\theta, \theta_o, \sigma)$ (with a unity integral)

$$f(\theta, \theta_o, \sigma) = \frac{1}{\sqrt{2\pi}\sigma} \cdot \exp\left(-\frac{1}{2} \cdot \left[\frac{\theta - \theta_o}{\sigma}\right]^2\right), \qquad (11)$$

where σ is the orientation bandwidth parameter of the tuning curve centered on peak orientation θ_o.

The weighting function of the inhibitory interaction applies onto the response of the linear input stage (Eq. (10)) according to the equation

$$r_i(\theta_i, \theta_s) = k \cdot \sum_{\theta} f(\theta, \theta_i, \sigma_i) \cdot r_e(\theta, \theta_s)^p, \qquad (12)$$

where k is the gain factor, σ_i the orientation bandwidth parameter, and θ_i the peak orientation of the inhibitory input. Note that we consider an inhibition applied onto the excitatory distribution r_e after a power law of index p, rather than directly on the stimulus (as visual input to cortex is mainly excitatory). The component r_i may then be seen as the response of a second-order inhibitory neuron (or interneuron), while r_e may be seen as the response of a first-order neuron.

2.5.2.4. Quasi-linear model with center-surround opponency. As early studies have suggested the existence of lateral inhibition between orientation detectors (Blakemore, Carpenter, & Georgeson, 1970; Blakemore & Tobin, 1972; Carpenter & Blakemore, 1973; Sillito, 1975, 1979), we consider a linear model of orientation selectivity based on center-surround opponency (Fig. 4A), where the inhibitory surround provided by the input r_i suppresses the excitatory center provided by the input r_e, according to the equation (for linearity purpose we assume $p = 1$)

$$L(\theta_o, \theta_s) = r_e(\theta_o, \theta_s) - r_i(\theta_o, \theta_s). \qquad (13)$$

Note that both excitatory and inhibitory components are centered on the same peak orientation θ_o. This model introduces explicitly lateral inhibitory interactions in the orientation domain ($k \neq 0$ in Eq. (12)). Analogous to the DOG filter (difference of gaussians) in the spatial domain, an inhibitory surround broader and weaker than the excitatory center induces a Mexican-hat-shaped tuning curve that has the effect of sharpening orientation selectivity. In absence of surround opponency ($k = 0$ in Eq. (12)), the linear model collapses to a unimodal filter characterized by the excitatory component r_e

$$L(\theta_o, \theta_s) = r_e(\theta_o, \theta_s). \qquad (14)$$

The response of this linear input stage per se is not appropriate as a model of the visual responses found in cortical neurons. It lacks two essential properties, response rectification and saturation, which we implement to form the quasi-linear models. Response rectification is implemented through a half-wave rectification

$$C(\theta_o, \theta_s) = \text{Max}[L(\theta_o, \theta_s), 0], \qquad (15)$$

while response saturation is incorporated in the model using a Naka–Rushton equation ($c^n/[c^n + \sigma^n]$) which has been shown to provide a good fit to the contrast response function of striate cortex neurons (Albrecht, Farrar, & Hamilton, 1984; Albrecht & Hamilton, 1982; Geisler & Albrecht, 1997; Sclar, Maunsell, & Lennie, 1990; Tolhurst & Heeger, 1997). We replace the contrast signal by the response of the linear input stage to form an orientation-selective quasi-linear model

$$R(\theta_o, \theta_s) = \frac{R_{\max} \cdot C(\theta_o, \theta_s)^n}{C(\theta_o, \theta_s)^n + \sigma_{1/2}^n} + M, \qquad (16)$$

where $R_{\max}$ is the maximum response, M is a spontaneous firing rate, $\sigma_{1/2}$ is the half-saturation constant, and n is the response exponent. Note that $C(\theta_o, \theta_s)$ is simply scaled by contrast due to the linearity of the input stage. The nonlinearity performed by this equation is a static energy gain control.

2.5.2.5. Nonlinear model with divisive inhibition. Evidence for a nonlinear contribution in the emergence of orientation tuning is numerous (Gardner, Anzai, Ohzawa, & Freeman, 1999). A modification of the Naka–Rushton equation, in which the energy response of orientation-selective filters replaces contrast and $\sigma_{1/2}$ is a globally pooled activity, has been proposed to account for the normalization of striate cell responses with respect to stimulus contrast (Heeger, 1992). This contrast-normalization model has been thought to be a critical feature of V1 cells to account for the contrast invariance of their orientation tuning (Sclar & Freeman, 1982; Skottun, Bradley, Sclar, Ohzawa, & Freeman, 1987). By considering the half-saturation constant $\sigma_{1/2}$ as a dynamic parameter, this idea of dynamic gain control has been further developed to account for the adaptive spatiotemporal control of visual sensitivity in the retina (Beaudot, 1994, 1996). Here, we propose a variation of the biophysical normalization model of Carandini and Heeger (Carandini & Heeger, 1994; Carandini, Heeger, & Movshon, 1999), in which $\sigma_{1/2}$ is a locally pooled activity that is orientation selective. The response of the nonlinear detector (Fig. 4B) centered on orientation θ_o is defined by a modified Naka–Rushton equation

$$R(\theta_o, \theta_s) = \frac{R_{\max} \cdot r_e(\theta_o, \theta_s)^p}{r_e(\theta_o, \theta_s)^p + r_i(\theta_o, \theta_s)^q} + M, \qquad (17)$$

where $r_e(\theta_o, \theta_s)$ and $r_i(\theta_o, \theta_s)$ are the excitatory and inhibitory input components, respectively (given by Eqs. (10) and (12)), $R_{\max}$ is the maximum response, power law indices p and q indicate the steepness of the excitatory and inhibitory components, respectively, and

M is a spontaneous firing rate. The component $r_i(\theta_o, \theta_s)^q$ is the signal strength at which the detector reaches half its maximum response. It is a dynamic and orientation-selective component that depends on the weighting of the neighboring filters' responses and that acts as a dynamic gain control through divisive inhibition.

2.5.2.6. Prediction for orientation discrimination. We assume that orientation discrimination is subserved by the differential response of a single detector. A change in orientation, $\Delta\theta$, across two stimulus intervals is detected when the differential response of a detector exceeds a response threshold ΔR. The response threshold ΔR is an unknown and subjective threshold parameter. A more objective criteria is provided by the ideal-observer theory which predicts the orientation discrimination performance of the model according to the formula (Geisler & Albrecht, 1997; Scobey & Gabor, 1989)

$$
d' = \frac{|\Delta Mean|}{\sqrt{AverageVariance}}
$$
$$
= |R(\theta_o, \theta_s + \Delta\theta)
$$
$$
- R(\theta_o, \theta_s)| \Big/ \sqrt{\frac{K \cdot R(\theta_o, \theta_s + \Delta\theta) + K \cdot R(\theta_o, \theta_s)}{2}} \quad (18)
$$

relating the discrimination index d' (1.0 for 75% correct in 2AFC) to the mean and standard deviation of the neural response in the presence of multiplicative noise, when the variance is proportional to the mean response by a constant K (typically with values between 1.2 and 1.5, we set K to 1.2 in the simulations). Orientation discrimination threshold can be derived from this formula by setting d' to 1.0 and solving for $\Delta\theta$ as function of stimulus bandwidth (σ_θ).

Note that stimulus peak orientation θ_s is a free parameter in Eq. (18) (as stated earlier we assume a vertical detector, i.e., $\theta_o = 90$ deg). The off-looking strategy suggests that the most sensitive part of the detector's response curve, at a remote orientation θ_{disc}, underlies orientation discrimination (note that it also depends on the stimulus orientation bandwidth parameter σ_θ). The remote orientation corresponds to the point of highest derivative where the slope of the tuning curve is the steepest, which is defined by

$$
|\partial_{\theta_s} R(\theta_o, \theta_{disc})| = \text{Max}_{\theta_s} \left| \frac{\partial R(\theta_o, \theta_s)}{\partial \theta_s} \right|. \quad (19)
$$

The discrimination index d' (Eq. (18)) can be approximated around the orientation (θ_{disc}) according to

$$
d'(\theta_{disc}) \approx \frac{2\Delta\theta \cdot |\partial_{\theta_s} R(\theta_o, \theta_{disc})|}{\sqrt{K \cdot R(\theta_o, \theta_{disc})}} \quad (20)
$$

and the orientation threshold (for $d' = 1$) is then given by

$$
\Delta\theta_{min} = \frac{1}{2} \cdot \frac{\sqrt{K \cdot R(\theta_{disc})}}{|\partial_\theta R(\theta_{disc})|}. \quad (21)
$$

We use this expression to predict the orientation discrimination threshold as function of the stimulus orientation bandwidth (σ_θ) for all models, and to fit them to the experimental data.

2.6. Fitting

We use Matlab (The MathWorks) and C programming to fit the various models to the threshold data using a least-squares weighted procedure and the Nelder–Mead simplex optimization combined with an iterative procedure (a simplified version of the "simulated annealing" method for global optimization) to verify the stability of the solution. The goodness of the fits is quantified with a Q measure. Q is a χ^2 distribution function that gives the probability that the minimum χ^2 is as large as it is purely by chance. For small Q values, the deviation from the model is unlikely to be due to chance and the model may be incorrect. For larger Q values, the deviation from the model is more likely to arise by chance suggesting the model is an adequate description of the data. A Q of 0.1 suggests an acceptable model fit (Press, Teukolsky, Vitterling, & Flannery, 1992).
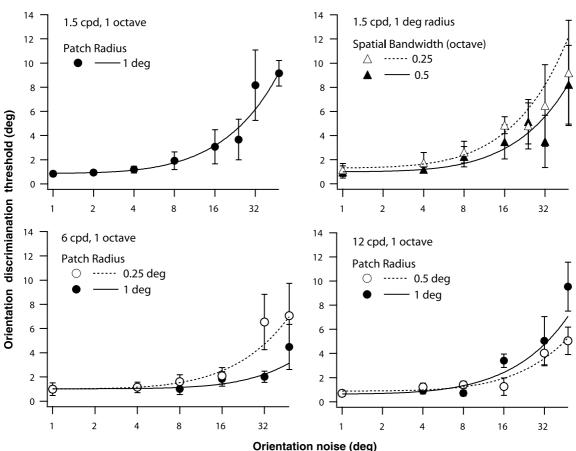
3. Results

3.1. Psychophysical measurement

Figs. 5 and 6 show the orientation thresholds (mean and standard deviation) measured for two subjects (WB and KTM) as a function of orientation bandwidth for various combinations of spatial frequency ($f_o = 1.5$–12 cpd), spatial bandwidth ($\sigma_f = 0.25$–1 octaves), and size ($\sigma_r = 0.25$–1 deg) of the stimuli. All data sets for both subjects are characterized by a monotonic increase of the orientation discrimination thresholds (σ_o) with the increase of stimulus bandwidth (σ_θ), and are successfully fitted with the variance summation model (Eq. (7)). This is a robust result consistent with previous studies (Beaudot & Mullen, 2002, 2005; Demanins et al., 1999; Heeley et al., 1997) which supports the idea that stimulus orientation bandwidth acts as a source of external noise.

The variance summation model provides a very good fit in 13/14 conditions ($Q > 0.4$). Table 1 shows for both subjects the internal noise (σ_{Int}), relative sampling efficiency and bandwidth of the discrimination tuning (σ_{knee}) derived from the fitting procedure (Eqs. (7) and (8)). We find no significant effect of the spatial bandwidth, spatial frequency, or size of the stimuli on internal noise and discrimination tuning. Table 1 shows the averaged parameters along the respective dimensions and across all conditions for each subject. Overall, internal orientation noise is about 0.9 ± 0.3 deg; the bandwidth parameter (σ_{knee}) of the orientation discrimination tuning is about 6.2 ± 2 deg, while sampling efficiency is more variable across conditions for both subjects (with subject KTM showing an overall higher relative efficiency). These estimates are in agreement with previous studies of orientation discrimination (Demanins et al., 1999; Heeley et al., 1997; Reisbeck & Gegenfurtner, 1998; Webster et al., 1990; Wuerger & Morgan, 1999).

The absence of an effect of spatial frequency or size on orientation discrimination is consistent with studies using circular patches of sinusoidal gratings that report that thresholds fall to asymptotic values as size, spatial frequency, and contrast increase (Burr & Wijesundra, 1991; Henrie & Shapley, 2001; Mareschal & Shapley, 2004). The stimuli parameters we used are in the range where this asymptotic behavior prevails. Note that varying the size (Henrie & Shapley, 2001; Mareschal & Shapley, 2004) or aspect ratio (Heeley & Buchanan-Smith, 1998) of the stimuli acts on their orientation bandwidth,

Measured Orientation Discrimination Thresholds

- Subject WB -

Fig. 5. Orientation discrimination threshold as a function of stimulus bandwidth for subject WB for various combinations of spatial bandwidth (0.25 and 0.5 octaves in top-right graph, 1 octave in all other graphs), spatial frequency (1.5–12 cpd), and size (radius of 0.25–1 deg). Error bars denote standard deviations. Smooth curves denote fits from the variance summation model.

for example decreasing the size or the height-to-width ratio broadens the stimulus orientation bandwidth.

The acute orientation acuity and the narrow tuning found for discrimination (full-bandwidth at half-height of about 15 deg) contrast with the broad orientation tuning of the detection mechanisms revealed by psychophysics and neurophysiology (3–5 times broader). In the next section, we investigate the ability of broadly tuned detectors to predict acute orientation acuity and discrimination threshold elevation with stimulus orientation bandwidth.

3.2. Simulations

This section presents the orientation properties of the quasi-linear and nonlinear models based on numerical simulations in response to the same patches of 2D orientation noise that we used psychophysically. Each stage is analyzed in terms of the orientation tuning and amplitudes of their responses as a function of the amount of external orientation noise (quantified by the orientation

bandwidth of the stimuli characterized by σ_θ), and are described by the qualitative effects of the various parameters on these properties. The ability of each model to account for psychophysical orientation discrimination is evaluated by deriving its orientation thresholds from Eq. (21) as a function of stimulus bandwidth. Next we demonstrate that the nonlinear model, based on a divisive broadband inhibition, is a more robust candidate than the quasi-linear models crippled by their contrast dependence.

3.2.1. Quasi-linear models

Fig. 7 illustrates the properties of the opponent quasi-linear model Eqs. (12)–(16) in terms of orientation tuning (Figs. 7A–C) and maximum amplitudes (Figs. 7B–D) for the response and its differentiation to stimuli normalized in terms of maximum contrast. In this example, the orientation inhibitory surround is characterized by a broad orientation tuning ($\sigma_i = 25$ deg) and a strong weight ($k = 1$), while the excitatory input is characterized by a narrower orientation tuning ($\sigma_e = 12$ deg). Solid, dotted,

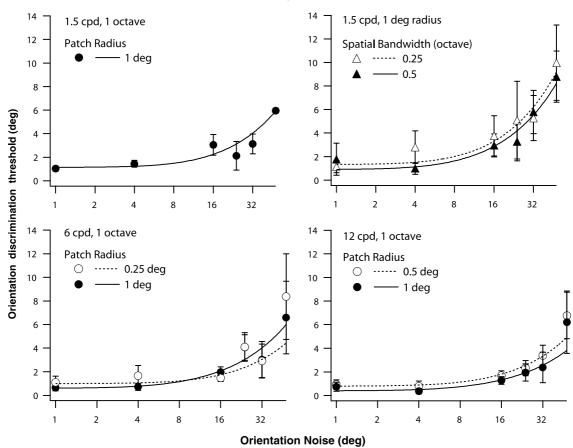**Measured Orientation Discrimination Thresholds**

- Subject KTM -

Fig. 6. Orientation discrimination threshold as a function of stimulus bandwidth for subject KTM. See Fig. 5 for details.

Table 1
Variance summation model's parameters

Parameters	WB				KTM			
	σ_f	f_o	σ_r	All	σ_f	f_o	σ_r	All
σ_{Int} (deg)	1 ± 0.2	0.8 ± 0.2	0.9 ± 0.1	0.9 ± 0.2	1.1 ± 0.2	0.7 ± 0.3	0.8 ± 0.3	0.9 ± 0.3
Efficiency	26 ± 8	112 ± 106	62 ± 40	43 ± 22	43 ± 18	97 ± 44	103 ± 36	82 ± 44
σ_{knee} (deg)	5.1 ± 0.5	8.4 ± 5.7	7.5 ± 4.3	5.1 ± 1.6	7.2 ± 1.6	6.4 ± 2.1	7.6 ± 2.4	7.2 ± 2.2

Means and standard deviations of the variance summation model's parameters (internal noise σ_{Int}, relative sampling efficiency, and knee point σ_{knee}) along the respective dimensions of the noise stimuli (spatial bandwidth parameter σ_f, spatial frequency f_o, and radius σ_r) and across all conditions for both subjects.

and dashed curves in Fig. 7A show the model's response to a range of stimulus bandwidths ($\sigma_\theta = 1$, 21, and 41 deg) as a function of the stimuli orientation peak, θ_s. The dash-dotted curve represents the Gaussian tuning curve of the Gabor filter with $\sigma_e = 12$ deg and centered on $\theta_o = 90$ deg. For all stimulus bandwidths, the quasi-linear model responds best to stimuli centered on the excitatory tuning ($\theta_s = \theta_o$), while the response decreases for stimuli centered on orientations further away. The main effect of increasing stimulus orientation bandwidth is a weakening and broadening in the orientation tuning

of the quasi-linear model output, the response tuning to the narrower stimuli being close to the filter tuning (defined by σ_e). Fig. 7B shows that the maximum response (obtained for stimuli centered on the excitatory tuning) is a monotonic function decreasing with stimulus bandwidth, which indicates that the quasi-linear model is more sensitive to narrow stimuli.

We assume that orientation discrimination is subserved by the differential response of the orientation-selective mechanism. Fig. 7C shows the differential response of the opponent quasi-linear model to a small change in
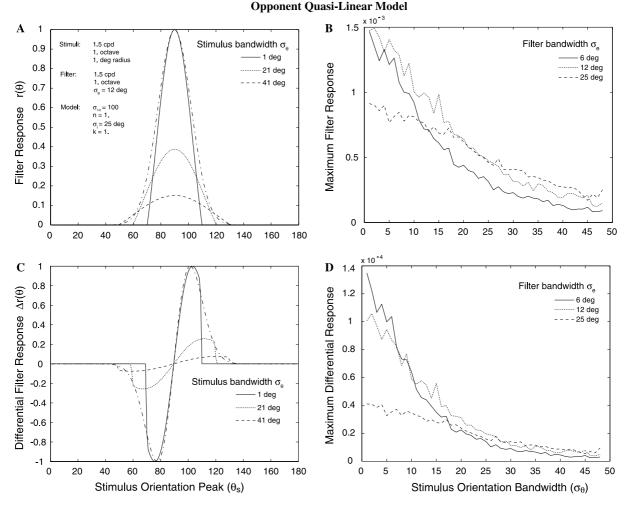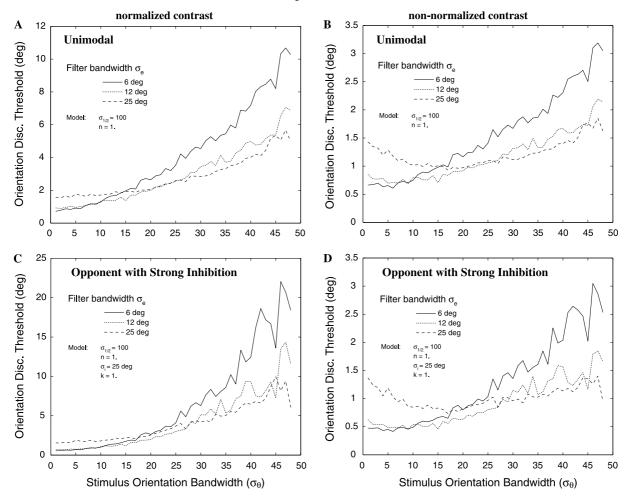
Opponent Quasi-Linear Model

Fig. 7. Properties of the opponent quasi-linear model (with strong inhibition, $k = 1$) as a function of orientation bandwidth (σ_θ) for contrast-normalized stimuli. (A) Orientation tuning of the filter response $R(\theta)$; (B) maximum detector's response; (C) orientation tuning of the detector's differential response $\partial R(\theta)/\partial \theta$; (D) maximum differential response. Dash-dot curves in A and C represent the filter orientation tuning ($\theta_o = 90$ deg). Solid, dotted, and dashed curves in (A) and (C) represent the responses at different stimulus orientation bandwidths. Solid, dotted, and dashed curves in (B) and (D) represent the maximum responses for different values of the filter orientation bandwidth.

the stimuli orientation ($\theta_s \rightarrow \theta_s + \Delta\theta$, with $\Delta\theta = 1$ deg) for different stimulus bandwidths (solid, dotted, and dashed curves). Consistent with the opponent-process model suggested by Regan and Beverley (1985) for orientation discrimination, the differential response is minimum for stimuli centered on the filter orientation ($\theta_s = \theta_o$) and the orthogonal orientation ($\theta_s = \theta_0 \pm 90$ deg), and reaches a maximum at neighboring orientations where the flanks of the filter tuning curve are the most sensitive to a change in stimulus orientation (Regan & Beverley, 1985). Both amplitude and orientation tuning of the differential response are modulated by the stimulus orientation bandwidth similarly to the model response: increasing the stimulus bandwidth weakens and broadens the orientation tuning of the differential response, which is similar to the Gabor filter's differential tuning for the narrowest stimuli (dash-dotted curve). Moreover the stimulus orientation providing the highest differential response (the

one we note θ_{disc} in Section 2) increases with the stimulus bandwidth. As depicted in Fig. 7D, the maximum differential response (obtained for $\theta_s = \theta_{disc}$) is a monotonically decreasing function with stimulus bandwidth, whose maximum (at $\sigma_\theta = 0$ deg) and steepness increase for Gabor filters with narrower bandwidth (σ_θ). This indicates that the narrower the Gabor filter, the more sensitive the quasi-linear model is to orientation change in narrow stimuli, but this advantage is lost for broader stimuli. Interestingly, this property is unaffected by the inhibition weight and the presence of the weak nonlinearities following the linear stage (half-wave rectification and compression) since the properties of the linear input stage (with and without surround inhibition) are qualitatively similar to those of the quasi-linear model. Except for a difference in responses scale, the amplitudes and tunings of the linear input stage are virtually the same as their quasi-linear counterparts.

**Predicted Orientation Discrimination Thresholds
for the Quasi-Linear Models**

Fig. 8. Predicted orientation discrimination thresholds for the quasi-linear models as function of stimulus bandwidth for different bandwidths of the linear input stage: (A) unimodal model for contrast-normalized stimuli; (B) unimodal model for stimuli with increasing contrast; (C) opponent model ($k = 1$, $\sigma_i = 25$ deg) for contrast-normalized stimuli; (D) opponent model ($k = 1$, $\sigma_i = 25$ deg) for stimuli with increasing contrast.

The quasi-linear model has the best response to stimuli with the narrowest orientation bandwidth, and this is a critical property for predicting an increase in orientation discrimination thresholds as function of stimulus orientation bandwidth, as reported psychophysically in Figs. 5 and 6. Broadening stimulus bandwidth has the effect of attenuating the amplitude and broadening the tuning of the differential response, increasing orientation discrimination thresholds as a consequence since they are assumed to be directly dependent on the orientation sensitivity of the underlying detectors. The strictly monotonic dependence of the differential response on stimulus bandwidth predicts that thresholds for orientation discrimination also monotonically increase as a function of the stimulus bandwidth. Applying the ideal-observer theory (Eq. (18)) to the quasi-linear model's response provides estimates of orientation discrimination thresholds (Fig. 8) comparable with their psychophysical counterparts (Figs. 5 and 6). As predicted by

the differential response, thresholds for the quasi-linear model rise monotonically with orientation noise when stimuli are contrast normalized (Figs. 8A and C). An analysis of the effects of the various parameters shows that: (i) the internal orientation noise rises with the bandwidth of the excitatory input stage (σ_e), the half-saturation constant ($\sigma_{1/2}$), and the response exponent (n), while it decreases with the bandwidth of the inhibitory surround (σ_i) and is unaffected by the inhibition weight (k); (ii) the acceleration of the Threshold versus Noise function (TvN) increases with the half-saturation constant, the inhibition weight, and the response exponent.

The above properties apply to the response of linear or quasi-linear models when their visual inputs are normalized in terms of maximum contrast. Figs. 8B and D show their properties when stimuli are not normalized, that is when their contrast covaries with their orientation bandwidth. In this condition, the predicted thresholds

for the quasi-linear model can be characterized by a U-shape function, more pronounced for input filters with a broad orientation bandwidth (for example, $\sigma_e = 25$ deg). This nonmonotonic relationship directly results from the linear dependence of the input stage on stimulus contrast. When contrast covaries with orientation noise (σ_θ), the maximum filter response and the maximum differential response are no longer decreasing monotonically. Instead, the maximum filter response increases monotonically with stimulus bandwidth and the maximum differential response shows an inverse U-shape with stimulus bandwidth. Neither the inhibition, half-wave rectification or compression corrects for this contrast dependence.

This behavior is clearly inconsistent with the effect of stimulus orientation bandwidth on orientation thresholds reported psychophysically in Figs. 5 and 6 or in previous studies, suggesting that the monotonic increase in orienta-

tion thresholds with stimulus bandwidth is contingent on contrast normalization already present in the stimuli. However, the existence of a nonmonotonic relation between threshold and noise is not supported by the psychophysical results shown in Fig. 9 for both subjects, in which stimulus contrast was increased with stimulus bandwidth instead of using normalized contrast. This control experiment shows no evidence of improved orientation discrimination for intermediate levels of orientation noise. Psychophysical orientation discrimination thresholds still show a monotonic increase with orientation noise despite increasing contrast. Moreover, as shown in Fig. 8 increasing contrast with stimulus bandwidth considerably improves orientation discrimination thresholds (note the different y-scales for the normalized versus non-normalized contrast conditions), a prediction refuted by the psychophysical measurements (compare Fig. 9 and Figs. 5 and 6).

To summarize, both linear and quasi-linear models predict a monotonic increase of orientation discrimination threshold with stimulus orientation noise when stimuli are normalized in terms of maximum contrast. However, these models fail to maintain the monotonic TvN function when stimulus contrast covaries with the amount of orientation noise. This shortcoming suggests that contrast normalization is required to achieve a monotonic increase of orientation thresholds with orientation noise. With stimuli contrast increasing with orientation noise, the nonmonotonic dependence of the differential response on stimulus bandwidth (described by an inverse U-shape) suggests that for the quasi-linear model a given threshold response for orientation discrimination can be reached for both small orientation changes in broadband stimuli (large σ_θ) and larger orientation changes in narrowband stimuli (small σ_θ). To achieve a response that decreases with stimulus bandwidth independently of contrast, the responses to narrowband and broadband stimuli need to be differently affected by the activity of neighboring filters; small response (to narrow stimuli) should be enhanced and large response (to broad stimuli) should be decreased according to the neighbors' activity. Intuitively, some context-dependent gain control in the orientation domain is required to achieve the relative enhancement of center activity and suppression of surround activity and to obtain a response similar to the response of the quasi-linear model to contrast-normalized stimuli (Fig. 7). The nonlinear model based on a broadband divisive inhibition and presented in the next section aims to achieve this goal. While the quasi-linear model has the same limitation as the linear input stage in terms of contrast dependence, it is useful because it is characterized by the same neural constraints as the nonlinear model (in terms of response expansion, saturation, gain, and spontaneous response) to which it can be readily compared in terms of predicted thresholds and fitted parameters.
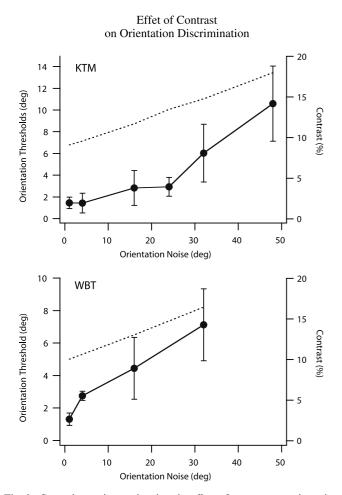

Fig. 9. Control experiment showing the effect of contrast on orientation discrimination thresholds as a function of stimulus bandwidth for two subjects. Results are shown for one stimulus condition (1 octave, 1.5 cpd, radius of 1 deg). Left y-axis and solid line denote orientation thresholds, while right y-axis and dotted line denote the contrast dependence with the orientation noise. Error bars denote standard deviations of the orientation thresholds.

Nonlinear Model

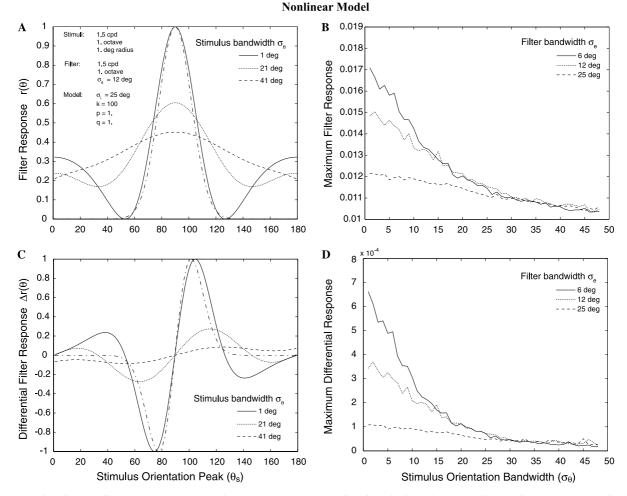

Fig. 10. Properties of the nonlinear model ($\sigma_i = 25$ deg, $k = 100$, $p = 1$, $q = 1$) as a function of orientation bandwidth (σ_θ) for contrast-normalized stimuli. See Fig. 7 for details.

3.2.2. Nonlinear model

We apply the same analysis to the nonlinear model characterized by a broadband divisive inhibition in the orientation domain, as given by Eq. (17) and illustrated in Fig. 4B. Fig. 10 presents the properties of this nonlinear model in terms of orientation tuning (Figs. 10A–C) and maximum amplitudes (Figs. 10B–D) for the response and its differentiation to stimuli normalized in terms of maximum contrast. In this example, orientation inhibitory surround is characterized by a broad orientation tuning ($\sigma_i = 25$ deg). The orientation tuning for the nonlinear model is qualitatively similar to the tuning of the opponent quasi-linear model (and its opponent input stage) with weak surround inhibition. Its tuning is characterized by a Mexican-hat shape for the narrower stimulus bandwidth (low noise levels) that changes to a broad unimodal tuning for broader stimulus bandwidths (high noise levels). It is noteworthy that the response tuning to the narrowest stimuli closely matches the tuning of the excitatory input (dash-dotted curve, σ_e). Both maximum response and maximum differential response (Figs. 10B and D) are characterized by a similar monotonic decrease with

stimulus orientation bandwidth: maximum amplitudes decrease more steeply for narrower input stage (small σ_e), and collapse to similar responses at high levels of orientation noise.

Applying the ideal-observer theory Eqs. (18)–(21) to the nonlinear model's response predicts monotonically increasing orientation discrimination thresholds with orientation noise (Fig. 11) comparable to the psychophysical counterparts. An analysis of the effects of the parameters shows that: (i) similar to the quasi-linear model, internal orientation noise worsens with the bandwidth of the excitatory input (σ_e), but improves with the inhibition bandwidth of the divisive input (σ_i). (ii) The acceleration of the *TvN* function drops with the bandwidth of both inputs. (iii) Thresholds increase with the weighting factor (k) and the response exponent (q) of the divisive inhibition, but decrease with the response exponent (p) of the excitatory input. It is essential to note that this monotonic relationship also holds for nonnormalized contrast because of the nature of Eqs. (12) and (17) (replace r_e by $c.r_e$ where c would be contrast). Note also that the responses are contrast invariant for $q = 1$ in Eq. (17),

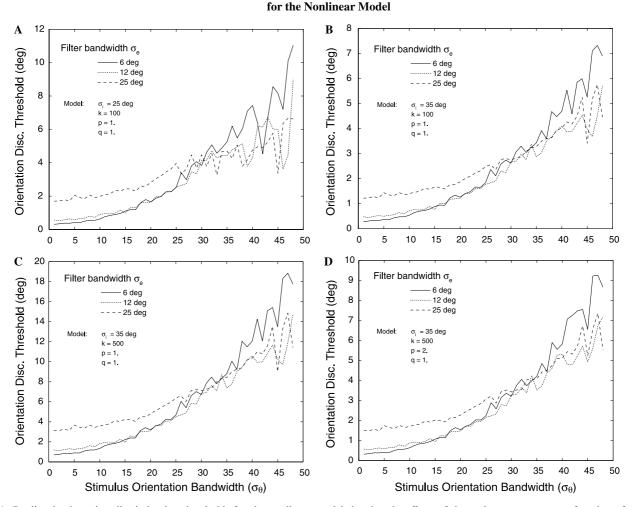**Predicted Orientation Discrimination Thresholds
for the Nonlinear Model**

Fig. 11. Predicted orientation discrimination thresholds for the nonlinear model showing the effects of the various parameters as function of stimulus bandwidth for different bandwidths of the linear input stage: (A) thresholds derived from responses presented in Fig. 10 ($\sigma_i = 25$ deg, $k = 100$, $p = 1$, $q = 1$); (B) increase in inhibitory bandwidth ($\sigma_i = 35$ deg, $k = 100$, $p = 1$, $q = 1$); (C) increase in inhibition weight ($\sigma_i = 35$ deg, $k = 500$, $p = 1$, $q = 1$; (D) increase in excitatory response exponent ($\sigma_i = 35$ deg, $k = 500$, $p = 2$, $q = 1$).

and that for very small values of the inhibitory response exponent ($q \ll 1$) the nonlinear model collapses to the unimodal quasi-linear model (with $\sigma_{1/2} = 1$ and $n = p$). In conclusion, the nonlinear model does not suffer from the flaw that hampers the linear and quasi-linear models since it predicts a monotonic increase of orientation discrimination threshold with stimulus orientation noise independently of stimulus contrast.

In summary, both quasi-linear and nonlinear models capture the fundamental property reported psychophysically for orientation discrimination when using contrast-normalized stimuli: orientation discrimination thresholds increase monotonically with stimulus orientation bandwidth. However, only the nonlinear model with broadband divisive inhibition maintains this relationship when contrast increases with stimulus bandwidth. In contrast, the linear and quasi-linear models show non-monotonic *TvN* functions when contrast is not normalized, and predict much lower than measured thresholds.

Note that in both models, there is no single parameter that uniquely determines internal orientation noise or threshold acceleration contrary to the variance summation model. The next section presents the results of the procedure for fitting the experimental data to each model.

3.3. Model fitting

We fit the unimodal quasi-linear ($k = 0$), opponent quasi-linear ($k \neq 0$) and nonlinear models to the psychophysical thresholds as function of the external orientation noise shown in Figs. 5 and 6. The unimodal quasi-linear model provides a very good fit in 12/14 conditions ($Q > 0.3$), the opponent quasi-linear model an acceptable fit for all conditions ($Q >= 0.1$), and the nonlinear model an acceptable fit in 13/14 conditions ($Q >= 0.15$). Fig. 12 shows some examples of the threshold data fitted by each model.

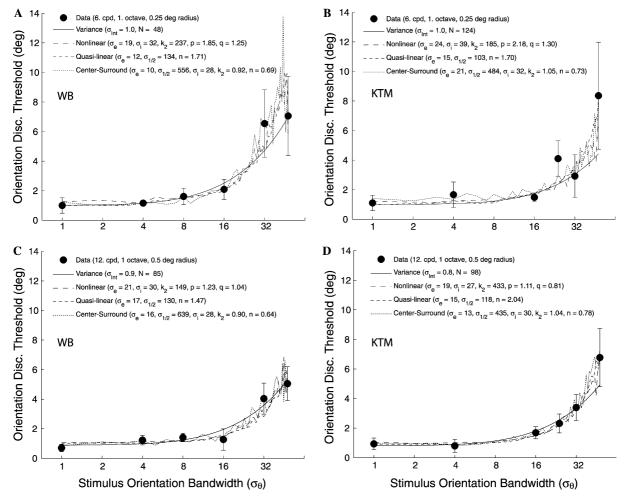**Fitted Orientation Discrimination Thresholds**

Fig. 12. Examples of fits obtained from the quasi-linear and nonlinear models. Symbols denote measured orientation discrimination thresholds as a function of stimulus bandwidth for subjects WB and KTM for various stimulus conditions (see Figs. 5 and 6). Error bars denote standard deviations. Solid, dotted, and dashed curves represent fits from the variance summation, quasi-linear and nonlinear models as indicated in the legends. Fitted parameters are indicated for each model.

Table 2
Unimodal quasi-linear model's parameters

Parameters	WB	KTM
σ_e (deg)	15.7 ± 5.1	14.6 ± 4.0
$\sigma_{1/2}^n$	148 ± 55	123 ± 39
n	1.7 ± 0.3	1.9 ± 0.3

Means and standard deviations of the unimodal quasi-linear model's parameters across all experimental conditions for both subjects: orientation bandwidth parameter of the excitatory input stage (σ_e), half-saturation constant ($\sigma_{1/2}$), and response exponent (n).

Table 2 shows the average and standard deviation of the parameters for the unimodal quasi-linear model across all experimental conditions. Orientation bandwidth, half-saturation constant, and response exponent are similar for the two subjects. The orientation half-bandwidth at half height of the linear input stage is about 17 ± 5 deg. The response exponent (n) is 1.8 ± 0.3, and the half-saturation constant ($\sigma_{1/2}^n$) is 135 ± 47.

Table 3
Opponent quasi-linear model's parameters

Parameters	WB	KTM
σ_e (deg)	14.9 ± 3.1	15.2 ± 3.8
σ_i (deg)	32.2 ± 9.4	35.3 ± 4.3
$\sigma_{1/2}^n$	486 ± 113	467 ± 131
n	0.70 ± 0.08	0.70 ± 0.05
k	0.93 ± 0.09	0.93 ± 0.13
σ_e/σ_i	0.51 ± 0.21	0.44 ± 0.12

Means and standard deviations of the opponent quasi-linear model's parameters across all experimental conditions for both subjects: orientation bandwidth parameters of the excitatory and inhibitory inputs (σ_e, σ_i), half-saturation constant ($\sigma_{1/2}$), response exponent (n), gain factor of the inhibitory input (k), and the ratio of the bandwidths (σ_e/σ_i).

Table 3 shows the average and standard deviation of the parameters for the opponent quasi-linear model across all experimental conditions. Orientation bandwidths, half-saturation constant, response exponent, and inhibitory weight

Table 4
Nonlinear model's parameters

Parameters	WB	KTM
σ_e (deg)	19.4 ± 3.7	19.7 ± 3.2
σ_i (deg)	30.9 ± 9.5	29.0 ± 4.7
p	1.4 ± 0.5	1.4 ± 0.4
q	1.1 ± 0.2	1.0 ± 0.2
k	175 ± 60	411 ± 190
σ_e/σ_i	0.7 ± 0.1	0.7 ± 0.1

Means and standard deviations of the nonlinear model's parameters across all experimental conditions for both subjects: orientation bandwidth parameters of the excitatory and inhibitory components (σ_e, σ_i), the power law indices of these components (p, q), the gain factor of the inhibitory component (k), and the ratio of the bandwidths (σ_e/σ_i).

are similar for the two subjects. The orientation half-bandwidths at half-height of the excitatory and inhibitory inputs are about 18 ± 4 and 40 ± 8 deg, respectively. The response exponent (n) is 0.7 ± 0.07, the half-saturation constant ($\sigma_{1/2}^n$) 476 ± 122, and the inhibitory weight (k) 0.93 ± 0.11. A parameter of particular interest is the ratio of the orientation bandwidths (σ_e/σ_i) which is 0.48 ± 0.16, indicating that the orientation tuning of the inhibitory input is on average about twice as large as the tuning of the excitatory input. Note the strong predicted inhibition ($k \approx 1$) and the low response exponent ($n < 1$).

Table 4 shows the average and standard deviation of the parameters for the nonlinear model across all experimental conditions. Orientation bandwidths and response exponents are similar for the two subjects. The orientation half-bandwidths at half-height of the excitatory and inhibitory inputs are about 23 ± 4 and 35 ± 8 deg, respectively. The exponents, p and q, are 1.4 ± 0.5 and 1.0 ± 0.2, respectively. The inhibitory weight (k) is more than twice larger for subject KTM (note that the variance summation model predicts a higher relative efficiency for this subject). The ratio of the orientation bandwidths (σ_e/σ_i) is 0.7 ± 0.1, indicating that the orientation bandwidth of the divisive input is about 40% larger than the bandwidth of the excitatory input.

Both quasi-linear models predict on average a relatively narrower orientation bandwidth for the excitatory input ($\sigma_e = 15 \pm 4$ deg) compared to the nonlinear model ($\sigma_e = 19.5 \pm 3.5$ deg). Both opponent quasi-linear and nonlinear models predict on average a relatively broad orientation bandwidth for the inhibitory input ($\sigma_i = 32 \pm 7$ deg). While the differences in bandwidths between the quasi-linear and nonlinear models do not appear statistically significant, the bandwidth ratios (σ_e/σ_i) seem to point towards a more significant effect: the opponent quasi-linear model predicts a linear center-surround interaction between a narrow excitatory and much broader inhibitory inputs, while the nonlinear model predicts a divisive center-surround interaction between excitatory and inhibitory inputs with much closer orientation tunings.

4. Discussion

We propose a new model for orientation discrimination that accounts for the robust monotonic increase of orientation thresholds with stimulus bandwidth acting as a source of external noise. First, this model challenges the validity of the variance summation model in the context of orientation processing, and second, it constitutes a biologically plausible alternative. Although cortical orientation selectivity has been one of the most studied aspects of visual processing, its origin and the role of cortical inhibition have been major issues of discordance in the vision community. Our model proposes that orientation sensitivity in orientation-tuned detectors results from a selective gain control mechanism in the orientation domain. This model, characterized by excitation and suppressive inhibition with relatively similar and broad orientation tuning, suggests that, rather than sharpening orientation tuning per se, intra-cortical mechanisms serve primarily to make orientation sensitivity less dependent on factors that are sources of uncertainty.

4.1. A challenge to the variance summation model?

The equivalent noise paradigm has been widely used to characterize the processing inefficiencies in the visual system, i.e., how external noise affects perceptual thresholds. Because perceptual thresholds generally increase monotonically with external noise, it has been proposed that they are determined by a summation of noise processes (Pelli, 1990; Pelli & Farell, 1999). By assuming the independence of these noise processes, the monotonic increase of thresholds with external noise is then simply predicted by a variance summation model (Eq. (7), Fig. 3). The conventional interpretation is that in high noise range performance is limited by external noise scaled by sampling efficiency, whereas the low noise range is associated with limitations due to (equivalent) internal noise, both revealing limitations in the observer's visual system. This threshold dependence on external noise generally holds for contrast sensitivity (Pelli & Farell, 1999). As orientation discrimination threshold increases monotonically with orientation noise, it has been assumed that the variance summation model also applies to orientation discrimination, and this model has been used to derive internal orientation noise and sampling efficiency of the mechanisms underlying orientation discrimination (Beaudot & Mullen, 2002, 2005; Demanins et al., 1999; Heeley et al., 1997). However, despite the empirical value of the equivalent noise paradigm for orientation processing, it has no theoretical ground yet in this context for several reasons.

First, models of contrast detection and discrimination assume nonlinear transducers that are monotonic with contrast (Kontsevich, Chen, & Tyler, 2002). Clearly, this

constraint does not apply to orientation sensitivity as the underlying detectors are orientation-tuned, and so nonmonotonic in their response to orientation. For example, an orientation-tuned detector produces exactly the same response to two gratings with different orientations if their contrasts are matched according to the tuning curve of the detector analogous to the principle of univariance in color vision. Second, contrary to the nonlinear model, the circular nature of the orientation domain is not embedded in the variance summation model. Third, the response variability in cortical neurons is characterized by a multiplicative noise (variance proportional to the mean, Geisler & Albrecht, 1995), so the amount of noise in a detector's response is not fixed but depends on the stimulus orientation. While neural noise may be a source of additive internal noise in contrast processing, the assumptions underlying the variance summation model, that noise processes are additive and independent so their variances add linearly, are less likely to apply in the context of orientation processing. Consequently the meaningfulness of internal orientation noise and sampling efficiency remains unclear in this context.

Internal noise reflects the existence of an absolute threshold in the absence of external noise (i.e., narrowband grating stimulus), and so should reflect some intrinsic properties of the neural mechanisms underlying orientation discrimination. Previous studies have suggested that the slopes of the detector tuning curve and the response variability determine orientation discrimination thresholds in single neurons (Bradley et al., 1985, Bradley, Skottun, Ohzawa, Sclar, & Freeman, 1987; Geisler & Albrecht, 1997; Scobey & Gabor, 1989; Vogels & Orban, 1990). The different models support this view since the main effects of orientation noise are the attenuation and broadening of the orientation tuning of the response curves, both resulting in a decrease of the tuning steepness as shown in Figs. 7A and 10A. The elevation in orientation discrimination thresholds is a direct consequence of this loss in orientation sensitivity in the detectors responses. In absence of external noise, orientation discrimination is limited by the slope of the tuning curve of the mechanism, which then depends on the orientation bandwidths of the excitatory and inhibitory components: internal noise increases with σ_e and decreases with σ_i. However, other factors clearly affect internal noise as suggested by Eq. (21). The internal orientation noise directly results from the shape of the tuning curve (steepness and response amplitude) and the proportionality constant K (between the mean and the variance, which does not differ significantly between cortical cells (Geisler & Albrecht, 1995; Scobey & Gabor, 1989)), not its bandwidth per se. Orientation discrimination predicted by the nonlinear model remains acute despite moderate levels of external noise (stimulus orientation bandwidth) and the broad orientation tuning of the detection mechanism. This emphasizes the fact that orientation discrimination is poorly correlated to the detector bandwidth.

To summarize, the nonlinear model accounts well for the effect of the stimulus orientation bandwidth on orientation discrimination thresholds. However, rather than assuming variance summation, this model relies on known properties of the neural detectors thought to underlie orientation detection and discrimination.

4.2. Biological plausibility

Many aspects of the nonlinear model are well supported by physiological data. First, its linear input stage, with an orientation tuning of 40 deg (full bandwidth at half-height), is consistent with the broad orientation selectivity of cortical cells first demonstrated by Hubel and Wiesel (Hubel & Wiesel, 1959, 1962, 1968), and with an aspect ratio between 1 and 1.5 typical of simple cells (De Valois et al., 1982; Parker & Hawken, 1988). Second, the presence of lateral inhibition in the orientation domain through orientation-selective interactions between orientation detectors is established in the cortex (Blakemore et al., 1970; Blakemore & Tobin, 1972; Carpenter & Blakemore, 1973), and is thought to enhance orientation selectivity by sharpening the broad tuning of cortical inputs (Nelson & Frost, 1978; Sillito, 1975, 1979). This accounts for the "Mexican hat" tuning reported in some primate V1 neurons (De Valois et al., 1982; Ringach, Hawken, & Shapley, 1997), also found psychophysically (Motoyoshi & Kingdom, 2003; Ringach, 1998). As shown by the tuning curve of the nonlinear model (Fig. 10A), such "Mexican hat" tuning emerges without resorting to linear interactions between narrowly tuned excitation and broadly tuned inhibition. A dynamic version of the nonlinear model (unpublished data) also predicts a center-surround tuning that develops over time similarly to the dynamics of V1 cells recently reported by Ringach et al. (Ringach, Hawken, & Shapley, 2003; Shapley, Hawken, & Ringach, 2003). Third, this inhibition is suppressive and may account for the cross-orientation suppression found in primate cortical neurons (Bonds, 1989; DeAngelis, Robson, Ohzawa, & Freeman, 1992; Morrone, Burr, & Maffei, 1982; Petrov, Pigarev, & Zenkin, 1980) and in human vision (Burr & Morrone, 1987; Morrone & Burr, 1986; Snowden & Hammett, 1992). Fourth, unlike previous models of V1 simple cells, this inhibition is broadly tuned to orientation (Burr, Morrone, & Maffei, 1981; De Valois et al., 1982; Hata, Tsumoto, Sato, Hagihara, & Tamura, 1988; Kabara & Bonds, 2001; Morrone et al., 1982; Nelson & Frost, 1978), is centered on the same orientation as the excitatory component (Allison, Casagrande, & Bonds, 1995; Bonds, 1989; Ferster, 1986; Roerig & Chen, 2002; Sato, Katsuyama, Tamura, Hata, & Tsumoto, 1996; Weliky, Kandler, Fitzpatrick, & Katz, 1995), and has a roughly similar bandwidth to the excitation (Anderson, Carandini, & Ferster, 2000; Ferster, 1986; Martinez, Alonso,

Reid, & Hirsch, 2002). Finally, in the nonlinear model response amplitude and orientation selectivity are unaffected by contrast and so it accounts for the contrast invariance of psychophysical orientation discrimination at suprathreshold contrasts (Bowne, 1990; Nasanen, Kukkonen, & Rovamo, 1997; Skottun et al., 1987; Smith & Thomas, 1989) (but see Mareschal & Shapley, 2004). Many neurons in the striate cortex reach their maximum response at low-to-medium contrasts (Sclar & Freeman, 1982; Shevelev, Lazareva, Novikova, & Tikhomirov, 1985; Skottun et al., 1987) also providing contrast invariance. In summary, these physiological data point towards an orientation-selective mechanism generated at the earliest cortical level that receives similarly structured excitatory and inhibitory inputs. The data also argue for a nonlinear, broadly tuned and centered inhibition similar to the divisive inhibition embedded in the nonlinear model.

5. Conclusion

There is a great deal of evidence that area V1 is more than a bank of static oriented filters. Area V1 performs sophisticated and complex image processing, which cannot be reduced to an array of spatiotemporal linear filters. On the contrary, it appears to constitute a bank of dynamic and interacting oriented nonlinear filters under the influence of visual context (Gilbert & Wiesel, 1990). The nonlinear model we propose for orientation discrimination suggests a further refinement of the function of simple cells in area V1. First, it supports the idea that the nonlinear interaction between similar and broadly tuned excitatory and inhibitory inputs may neither creates nor sharpens orientation selectivity originating from a strong orientation-tuned thalamic input (Chung & Ferster, 1998; Ferster, 1987; Ferster, Chung, & Wheat, 1996; Nelson, Toth, Sheth, & Sur, 1994; Reid & Alonso, 1995), but rather makes simple cells selectively sensitive to one-dimensional stimuli such as contours (Burr et al., 1981; Morrone et al., 1982). Second, and more importantly, this orientation-selective intra-cortical inhibition may help to maintain their sensitivity to orientation change despite orientation uncertainty by ensuring that the orientation tuning is less dependent on internal and external factors that greatly vary from cell to cell and that are sources of orientation uncertainty, due to either stimulus bandwidth, variability in receptive field size and shape (Gardner et al., 1999), or contrast variance. However, it is unlikely to constitute the sole neural substrate underlying human performance. V1 cells show a high diversity of properties with a wide range of orientation tuning from very sharp to very broad (Mario, Schummers, & Sur, 2003; Monier, Chavane, Baudot, Graham, & Fregnac, 2003; Ringach, Shapley, & Hawken, 2002; Shevelev et al., 1985), while human vision is only characterized by broadly orientation-tuned detection mechanisms (Blake & Holopigian, 1985; Pandey Vimal, 1997; Phillips & Wilson, 1984). The present model also suggests that, while single neurons may reliably signal orientation discrimination (Geisler & Albrecht, 1995; Zohary, Hillman, & Hochstein, 1990) and may account for the orientation discrimination thresholds reported psychophysically, the underlying computation involves nonlinear interactions amongst a neural population with similar orientation tuning and overlapping receptive fields.

Appendix A. Simulation details

Because of the stochastic nature of the stimuli, their convolution with the Gabor filter (linear input stage) results in highly noisy responses. Averaging the filter responses on many stimuli generated with the same set of parameters provides a smoother response that can be used to fit the models to the experimental data. However, this scheme is extremely costly as the computation of a single instance for a given filter requires 180×48 (# stimulus orientations × # stimulus orientation bandwidths) calculations, each involving the generation of a stimulus (Fourier spectrum + inverse Fourier transform + product with a Gaussian envelope + normalization), followed by the convolution with the filter (Fourier transform + product with the filter spectrum + inverse Fourier transform) and the Max function (Eq. (10)). Fortunately, the filtering of each stimulus (with a given orientation bandwidth) shows a Gaussian distribution as function of the stimulus orientation, which can be fitted with the function

$$g(\theta) = b + a \cdot \exp\left(-\frac{1}{2} \cdot \left[\frac{\theta - \theta_o}{\sigma}\right]^2\right), \tag{A.1}$$

where b is the baseline, a is the amplitude, σ is the spread, and θ_o is the peak orientation of the Gaussian distribution (θ_o is constrained to the filter orientation). Coefficient of variation (rms error/mean) is less than 10% for all fits (i.e., all orientation bandwidths of filters and stimuli).

This computational shortcut is particularly valuable when fitting the models to the experimental data. As orientation bandwidth of the Gabor filter (σ_e) is a free parameter in this process, we pre-compute the response of the linear input stage to 180×48 stimuli configurations as function of the filter orientation bandwidth ($\sigma_e = 1$–45 deg by step of 1 deg). Then we fit the Gaussian distribution (Eq. A.1) to the 48×45 (# stimulus bandwidths × # filter bandwidths) responses of the input stage as function of stimulus orientation. Once pre-computed, the response of the 2D

linear input stage to any combination of stimulus orientation bandwidth (σ_θ), stimulus mean orientation (θ_o), and filter orientation bandwidth (σ_e) can feed the subsequent 1D stages of the models. Hence, pre-computing the most costly part of the simulation provides an effective way to fit all models to the experimental data.

References

Albrecht, D. G., Farrar, S. B., & Hamilton, D. B. (1984). Spatial contrast adaptation characteristics of neurones recorded in the cat's visual cortex. *The Journal of Physiology, 347*, 713–739.

Albrecht, D. G., & Hamilton, D. B. (1982). Striate cortex of monkey and cat: Contrast response function. *Journal of Neurophysiology, 48*(1), 217–237.

Allison, J. D., Casagrande, V. A., & Bonds, A. B. (1995). The influence of input from the lower cortical layers on the orientation tuning of upper layer VI cells in a primate. *Visual Neuroscience, 12*(2), 309–320.

Anderson, J. S., Carandini, M., & Ferster, D. (2000). Orientation tuning of input conductance, excitation, and inhibition in cat primary visual cortex. *Journal of Neurophysiology, 84*(2), 909–926.

Beaudot, W. H. A. (1994). *Le traitement neuronal de l'information dans la rétine des vertébrés: Un creuset d'idées pour la vision artificielle, PhD. thesis. Laboratoire TIRF* (p. 230). Grenoble: Institut National Polytechnique de Grenoble, France.

Beaudot, W. H. A. (1996). Sensory coding in the vertebrate retina: Towards an adaptive control of visual sensitivity. *Network: Computation in Neural Systems, 7*(2), 317–323.

Beaudot, W. H. A., & Mullen, K. T. (2002). Orientation selectivity in luminance and color vision assessed using 2-d bandpass filtered spatial noise. *Journal of Vision, 2*(7), 280a.

Beaudot, W. H. A., & Mullen, K. T. (2005). Orientation selectivity in luminance and color vision assessed using 2-d band-pass filtered spatial noise. *Vision Research, 45*(6), 687–696.

Blake, R., & Holopigian, K. (1985). Orientation selectivity in cats and humans assessed by masking. *Vision Research, 25*(10), 1459–1467.

Blakemore, C., Carpenter, R. H., & Georgeson, M. A. (1970). Lateral inhibition between orientation detectors in the human visual system. *Nature, 228*(5266), 37–39.

Blakemore, C., & Tobin, E. A. (1972). Lateral inhibition between orientation detectors in the cat's visual cortex. *Experimental Brain Research, 15*(4), 439–440.

Bonds, A. B. (1989). Role of inhibition in the specification of orientation selectivity of cells in the cat striate cortex. *Visual Neuroscience, 2*(1), 41–55.

Bowne, S. F. (1990). Contrast discrimination cannot explain spatial frequency, orientation or temporal frequency discrimination. *Vision Research, 30*(3), 449–461.

Bradley, A., Skottun, B. C., Ohzawa, I., Sclar, G., & Freeman, R. D. (1985). Neurophysiological evaluation of the differential response model for orientation and spatial-frequency discrimination. *Journal of the Optical Society of America A, 2*(9), 1607–1610.

Bradley, A., Skottun, B. C., Ohzawa, I., Sclar, G., & Freeman, R. D. (1987). Visual orientation and spatial frequency discrimination: A comparison of single neurons and behavior. *Journal of Neurophysiology, 57*(3), 755–772.

Burr, D., Morrone, C., & Maffei, L. (1981). Intra-cortical inhibition prevents simple cells from responding to textured visual patterns. *Experimental Brain Research, 43*(3–4), 455–458.

Burr, D. C., & Morrone, M. C. (1987). Inhibitory interactions in the human vision system revealed in pattern-evoked potentials. *The Journal of Physiology, 389*, 1–21.

Burr, D. C., & Wijesundra, S. A. (1991). Orientation discrimination depends on spatial frequency. *Vision Research, 31*(7–8), 1449–1452.

Carandini, M., & Heeger, D. J. (1994). Summation and division by neurons in primate visual cortex. *Science, 264*(5163), 1333–1336.

Carandini, M., Heeger, D. J., & Movshon, J. A. (1999). Linearity and gain control in V1 simple cells. In: *Models of cortical circuits* (Vol. 13, pp. 401–443).

Carpenter, R. H., & Blakemore, C. (1973). Interactions between orientations in human vision. *Experimental Brain Research, 18*(3), 287–303.

Chung, S., & Ferster, D. (1998). Strength and orientation tuning of the thalamic input to simple cells revealed by electrically evoked cortical suppression. *Neuron, 20*(6), 1177–1189.

Cole, G. R., & Hine, T. (1992). Computation of cone contrasts for color vision research. *Behavioural Research, Methods and Instrumentation, 24*, 22–27.

De Valois, R. L., Yund, E. W., & Hepler, N. (1982). The orientation and direction selectivity of cells in macaque visual cortex. *Vision Research, 22*(5), 531–544.

DeAngelis, G. C., Robson, J. G., Ohzawa, I., & Freeman, R. D. (1992). Organization of suppression in receptive fields of neurons in cat visual cortex. *Journal of Neurophysiology, 68*(1), 144–163.

Demanins, R., Hess, R. F., Williams, C. B., & Keeble, D. R. (1999). The orientation discrimination deficit in strabismic amblyopia depends upon stimulus bandwidth. *Vision Research, 39*(24), 4018–4031.

Ferster, D. (1986). Orientation selectivity of synaptic potentials in neurons of cat primary visual cortex. *The Journal of Neuroscience, 6*(5), 1284–1301.

Ferster, D. (1987). Origin of orientation-selective EPSPs in simple cells of cat visual cortex. *The Journal of Neuroscience, 7*(6), 1780–1791.

Ferster, D., Chung, S., & Wheat, H. (1996). Orientation selectivity of thalamic input to simple cells of cat visual cortex. *Nature, 380*(6571), 249–252.

Gardner, J. L., Anzai, A., Ohzawa, I., & Freeman, R. D. (1999). Linear and nonlinear contributions to orientation tuning of simple cells in the cat's striate cortex. *Visual Neuroscience, 16*(6), 1115–1121.

Geisler, W. S., & Albrecht, D. G. (1995). Bayesian analysis of identification performance in monkey visual cortex: Nonlinear mechanisms and stimulus certainty. *Vision Research, 35*(19), 2723–2730.

Geisler, W. S., & Albrecht, D. G. (1997). Visual cortex neurons in monkeys and cats: Detection, discrimination, and identification. *Visual Neuroscience, 14*(5), 897–919.

Gilbert, C. D., & Wiesel, T. N. (1990). The influence of contextual stimuli on the orientation selectivity of cells in primary visual cortex of the cat. *Vision Research, 30*(11), 1689–1701.

Hammond, P., & Andrews, D. P. (1978). Orientation tuning of cells in areas 17 and 18 of the cat's visual cortex. *Experimental Brain Research, 31*(3), 341–351.

Hata, Y., Tsumoto, T., Sato, H., Hagihara, K., & Tamura, H. (1988). Inhibition contributes to orientation selectivity in visual cortex of cat. *Nature, 335*(6193), 815–817.

Heeger, D. J. (1992). Normalization of cell responses in cat striate cortex. *Visual Neuroscience, 9*(2), 181–197.

Heeley, D. W., & Buchanan-Smith, H. M. (1998). The influence of stimulus shape on orientation acuity. *Experimental Brain Research, 120*(2), 217–222.

Heeley, D. W., Buchanan-Smith, H. M., Cromwell, J. A., & Wright, J. S. (1997). The oblique effect in orientation acuity. *Vision Research, 37*(2), 235–242.

Heggelund, P., & Albus, K. (1978). Orientation selectivity of single cells in striate cortex of cat: The shape of orientation tuning curves. *Vision Research, 18*(8), 1067–1071.

Henrie, J. A., & Shapley, R. M. (2001). The relatively small decline in orientation acuity as stimulus size decreases. *Vision Research, 41*(13), 1723–1733.

Hubel, D. H., & Wiesel, T. N. (1959). Receptive fields of single neurones in the cat's striate cortex. *The Journal of Physiology, 148*, 574–591.

Hubel, D. H., & Wiesel, T. N. (1962). Receptive fields, binocular interaction and functional architecture in the cat's visual cortex. *The Journal of Physiology, 160*, 106–154.

Hubel, D. H., & Wiesel, T. N. (1968). Receptive fields and functional architecture of monkey striate cortex. *The Journal of Physiology, 195*, 215–243.

Jones, J. P., & Palmer, L. A. (1987). An evaluation of the two-dimensional Gabor filter model of simple receptive fields in cat striate cortex. *Journal of Neurophysiology, 58*(6), 1233–1258.

Kabara, J. F., & Bonds, A. B. (2001). Modification of response functions of cat visual cortical cells by spatially congruent perturbing stimuli. *Journal of Neurophysiology, 86*(6), 2703–2714.

Kontsevich, L. L., Chen, C. C., & Tyler, C. W. (2002). Separating the effects of response nonlinearity and internal noise psychophysically. *Vision Research, 42*(14), 1771–1784.

Mareschal, I., & Shapley, R. M. (2004). Effects of contrast and size on orientation discrimination. *Vision Research, 44*(1), 57–67.

Mario, J., Schummers, J., & Sur, M. (2003). Combination of new electrophysiological and imaging techniques in the study of primary visual cortex function. *Revista de Neurologia, 36*(10), 944–950.

Martinez, L. M., Alonso, J. M., Reid, R. C., & Hirsch, J. A. (2002). Laminar processing of stimulus orientation in cat visual cortex. *The Journal of Physiology, 540*(Pt 1), 321–333.

Monier, C., Chavane, F., Baudot, P., Graham, L. J., & Fregnac, Y. (2003). Orientation and direction selectivity of synaptic inputs in visual cortical neurons: A diversity of combinations produces spike tuning. *Neuron, 37*(4), 663–680.

Morrone, M. C., & Burr, D. C. (1986). Evidence for the existence and development of visual inhibition in humans. *Nature, 321*(6067), 235–237.

Morrone, M. C., Burr, D. C., & Maffei, L. (1982). Functional implications of cross-orientation inhibition of cortical visual cells. I. Neurophysiological evidence. *Proceedings of the Royal Society of London. Series B. Biological Sciences, 216*(1204), 335–354.

Motoyoshi, I., & Kingdom, F. A. (2003). Orientation opponency in human vision revealed by energy-frequency analysis. *Vision Research, 43*(21), 2197–2205.

Nasanen, R. E., Kukkonen, H. T., & Rovamo, J. M. (1997). Modeling spatial integration and contrast invariance in visual pattern discrimination. *Investigative Ophthalmology and Visual Science, 38*(1), 260–266.

Nelson, J. I., & Frost, B. J. (1978). Orientation-selective inhibition from beyond the classic visual receptive field. *Brain Research, 139*(2), 359–365.

Nelson, S., Toth, L., Sheth, B., & Sur, M. (1994). Orientation selectivity of cortical neurons during intracellular blockade of inhibition. *Science, 265*(5173), 774–777.

Pandey Vimal, R. L. (1997). Orientation tuning of the spatial-frequency-tuned mechanisms of the red-green channel. *Journal of the Optical Society of America A, 14*(10), 2622–2632.

Parker, A. J., & Hawken, M. J. (1988). Two-dimensional spatial structure of receptive fields in monkey striate cortex. *Journal of the Optical Society of America A, 5*(4), 598–605.

Pelli, D. G. (1990). The quantum efficiency of vision. In C. B. Blakemore (Ed.), *Vision: Coding and efficiency* (pp. 3–24). Cambridge: Cambridge University Press.

Pelli, D. G., & Farell, B. (1999). Why use noise? *Journal of the Optical Society of America. A, Optics, image science, and vision, 16*(3), 647–653.

Petrov, A. P., Pigarev, I. N., & Zenkin, G. M. (1980). Some evidence against Fourier analysis as a function of the receptive fields in cats striate cortex. *Vision Research, 20*(11), 1023–1025.

Phillips, G. C., & Wilson, H. R. (1984). Orientation bandwidths of spatial mechanisms measured by masking. *Journal of the Optical Society of America A, 1*(2), 226–232.

Press, W. H., Teukolsky, S. A., Vitterling, W. T., & Flannery, B. P. (1992). *Numerical recipes in C: The art of scientific computing.* Cambridge: Cambridge University.

Regan, D., & Beverley, K. I. (1985). Postadaptation orientation discrimination. *Journal of the Optical Society of America A, 2*(2), 147–155.

Reid, R. C., & Alonso, J. M. (1995). Specificity of monosynaptic connections from thalamus to visual cortex. *Nature, 378*(6554), 281–284.

Reisbeck, T. E., & Gegenfurtner, K. R. (1998). Effects of contrast and temporal frequency on orientation discrimination for luminance and isoluminant stimuli. *Vision Research, 38*(8), 1105–1117.

Ringach, D. L. (1998). Tuning of orientation detectors in human vision. *Vision Research, 38*(7), 963–972.

Ringach, D. L., Hawken, M. J., & Shapley, R. (1997). Dynamics of orientation tuning in macaque primary visual cortex. *Nature, 387*(6630), 281–284.

Ringach, D. L., Hawken, M. J., & Shapley, R. (2003). Dynamics of orientation tuning in macaque v1: The role of global and tuned suppression. *Journal of Neurophysiology, 90*(1), 342–352.

Ringach, D. L., Shapley, R. M., & Hawken, M. J. (2002). Orientation selectivity in macaque V1: Diversity and laminar dependence. *The Journal of Neuroscience, 22*(13), 5639–5651.

Roerig, B., & Chen, B. (2002). Relationships of local inhibitory and excitatory circuits to orientation preference maps in ferret visual cortex. *Cerebral Cortex, 12*(2), 187–198.

Sankeralli, M. J., & Mullen, K. T. (1996). Estimation of the L-, M-, and S-cone weights of the postreceptoral detection mechanisms. *Journal of the Optical Society of America A, 13*(5), 906–915.

Sato, H., Katsuyama, N., Tamura, H., Hata, Y., & Tsumoto, T. (1996). Mechanisms underlying orientation selectivity of neurons in the primary visual cortex of the macaque. *The Journal of Physiology, 494*(Pt 3), 757–771.

Sclar, G., & Freeman, R. D. (1982). Orientation selectivity in the cat's striate cortex is invariant with stimulus contrast. *Experimental Brain Research, 46*(3), 457–461.

Sclar, G., Maunsell, J. H., & Lennie, P. (1990). Coding of image contrast in central visual pathways of the macaque monkey. *Vision Research, 30*(1), 1–10.

Scobey, R. P., & Gabor, AJ. (1989). Orientation discrimination sensitivity of single units in cat primary visual cortex. *Experimental Brain Research, 77*(2), 398–406.

Shapley, R., Hawken, M., & Ringach, D. L. (2003). Dynamics of orientation selectivity in the primary visual cortex and the importance of cortical inhibition. *Neuron, 38*(5), 689–699.

Shevelev, L. A., Lazareva, N. A., Novikova, R. V., & Tikhomirov, A. S. (1985). Standardness and invariability of the detector tuning of neurons in the orientation column of the visual cortex of the cat. *Neirofiziologiia, 17*(2), 175–182.

Sillito, A. M. (1975). The contribution of inhibitory mechanisms to the receptive field properties of neurones in the striate cortex of the cat. *The Journal of Physiology, 250*(2), 305–329.

Sillito, A. M. (1979). Inhibitory mechanisms influencing complex cell orientation selectivity and their modification at high resting discharge levels. *The Journal of Physiology, 289*, 33–53.

Skottun, B. C., Bradley, A., Sclar, G., Ohzawa, I., & Freeman, R. D. (1987). The effects of contrast on visual orientation and spatial frequency discrimination: A comparison of single cells and behavior. *Journal of Neurophysiology, 57*(3), 773–786.

Smith, B. G., & Thomas, J. P. (1989). Why are some spatial discriminations independent of contrast? *Journal of the Optical Society of America A, 6*(5), 713–724.

Snowden, R. J., & Hammett, ST. (1992). Subtractive and divisive adaptation in the human visual system. *Nature, 355*(6357), 248–250.

Swindale, N. V. (1998). Orientation tuning curves: Empirical description and estimation of parameters. *Biological Cybernetics, 78*(1), 45–56.

Tolhurst, D. J., & Heeger, D. J. (1997). Comparison of contrast-normalization and threshold models of the responses of simple cells in cat striate cortex. *Visual Neuroscience, 14*(2), 293–309.

Vogels, R., & Orban, G. A. (1990). How well do response changes of striate neurons signal differences in orientation: A study in the discriminating monkey. *The Journal of Neuroscience, 10*(11), 3543–3558.

Vogels, R., & Orban, G. A. (1991). Quantitative study of striate single unit responses in monkeys performing an orientation discrimination task. *Experimental Brain Research, 84*(1), 1–11.

Webster, M. A., De Valois, K. K., & Switkes, E. (1990). Orientation and spatial-frequency discrimination for luminance and chromatic gratings. *Journal of the Optical Society of America A, 7*(6), 1034–1049.

Weliky, M., Kandler, K., Fitzpatrick, D., & Katz, L. C. (1995). Patterns of excitation and inhibition evoked by horizontal connections in visual cortex share a common relationship to orientation columns. *Neuron, 15*(3), 541–552.

Wilson, H. R., & Regan, D. (1984). Spatial-frequency adaptation and grating discrimination: Predictions of a line-element model. *Journal of the Optical Society of America A, 1*(11), 1091–1096.

Wuerger, S. M., & Morgan, M. J. (1999). Input of long- and middle-wavelength-sensitive cones to orientation discrimination. *Journal of the Optical Society of America A, 16*(3), 436–442.

Zohary, E., Hillman, P., & Hochstein, S. (1990). Time course of perceptual discrimination and single neuron reliability. *Biological Cybernetics, 62*(6), 475–486.